ACS APPLIED ENGINEERING MATERIALS

pubs.acs.org/acsaenm Article

# $CO_2$ Capture with Capsules of Ionic Liquid/Amines

Luma Al-Mahbobi, Aidan Klemm, Cameron Taylor, Burcu Gurkan, and Emily Pentzer*

Cite This: *ACS Appl. Eng. Mater.* 2024, 2, 1298–1305 Read Online

ACCESS | Metrics & More | Article Recommendations | Supporting Information

**ABSTRACT:** Carbon capture remains an urgent issue that has gained a great deal of attention over the past few decades. Aqueous amines have excellent selectivity, but present corrosion and volatility issues, whereas ionic liquids (ILs) have negligible volatility and tunable physical properties, but high viscosities. One approach to improve the practical performance of these liquids is encapsulating them in a $CO_2$ permeable polymer shell to enhance the accessibility of the liquid and the $CO_2$ absorption rate. In this work, we report the encapsulation of a mixture of amine and IL (i.e., monoethanolamine (MEA) and 1-butyl-3-methylimidazolium tetrafluoroborate ([BMIM][$BF_4$])) and demonstrate enhanced carbon capture performance. A soft-template approach and interfacial polymerization are used to give capsules with liquid core (64 wt %) and polyurea shell. Compared to the bulk liquid, the encapsulated liquid shows improved thermal stability over cycles of absorption at 25 °C, and desorption at 75 °C. The capsules with core of [BMIM][$BF_4$]-MEA show 0.2 mol $CO_2$/kg of capsules at 1 bar $CO_2$, compared to the bulk liquid, which has 0.05 mol $CO_2$/kg of sorbent. This is attributed to the limited evaporation of the amines. Alternatively, the same capsules but with 5 wt % of piperazine (Pz) in the core have doubled gravimetric $CO_2$ capacity of the capsules (0.4 mol $CO_2$/kg of capsules); performance is evaluated over 10 capture–release cycles showing minimal mass loss. Characterization of the $CO_2$ uptake of the polymer shell itself reveals that the shell contributes only ∼10% of the observed capacity, likely attributed to amine functionalities of the polymer. This facile approach to encapsulating such "active" liquids can be applied to other $CO_2$ selective solvents that are volatile, viscous, and corrosive.

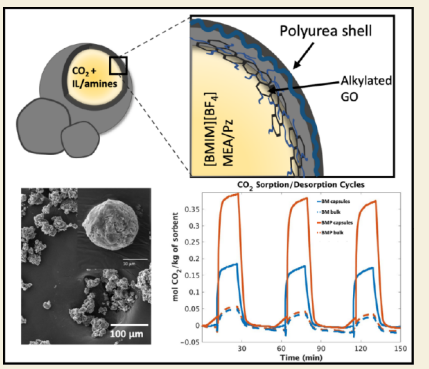


**KEYWORDS:** *carbon capture, ionic liquid, encapsulation, direct air capture, emulsion*



## INTRODUCTION

The rising level of $CO_2$ in the atmosphere due to the burning of fossil fuels, an essential source of energy that has yet to be matched, necessitates carbon capture to avoid catastrophic climate change. Traditional reliance on natural $CO_2$ sinks, like forests, is no longer sufficient, and thus to reach net-zero emissions, manmade $CO_2$-capture materials are required for not only flue gas separation but also for direct air capture (DAC).[1] To address this critical need, both solid-state materials and liquidous systems have been developed. Examples of solid-state porous adsorbents include zeolites and metal–organic frameworks (MOFs), which have high $CO_2$ selectivity, but are typically limited in application due to high cost and poor scalability.[2] In addition, mixed-matrix membranes (MMM) are composed of highly selective porous adsorbents in a tunable polymer matrix. This can create high-performance gas separation membranes, but these systems also face scalability issues.[3−7] Amine scrubbing, a patented technology developed in the 1930s, has been the primary method for capturing $CO_2$.[8] This method leverages a reaction between aqueous amines and $CO_2$ from flue gas, with the amines regenerated by stripping $CO_2$ at elevated temperatures, typically 100–120 °C.[9] Further, aqueous solutions of piperazine (Pz) and its mixture with monoethanolamine (MEA) have been shown to be a competitive alternative solvent in flue gas $CO_2$ capture due to faster kinetics attributed to Pz acting as a base, which accelerates reaction of $CO_2$ with alkanolamines.[10−14] Unfortunately, this method can be costly due to the evaporation of MEA, which has a high vapor pressure at desorption temperatures,[15] and water during regeneration, which requires the continuous addition of the solvent. Further, when used neat, amines experience severe viscosity increase upon $CO_2$ binding, and their corrosive nature leads to safety concerns and the need for infrastructure renewal.[16] Recent efforts have addressed the development of water-lean amine sorbents by strategically tuning hydrogen bonding within a liquid network.[17] The water-lean solvent approach provides an alternative for aqueous amines, while also promising to minimize the high energy costs associated with solvent regeneration due to their lower water content.[18,19]

In addition to liquid amines, ionic liquids (ILs) have recently received much attention for their use in carbon capture. ILs are salts that melt below 100 °C and are typically

Received: February 22, 2024
Revised: April 17, 2024
Accepted: April 19, 2024
Published: May 1, 2024




https://doi.org/10.1021/acsaenm.4c00118
*ACS Appl. Eng. Mater.* 2024, 2, 1298–1305

composed of a bulky organic cation and an organic or inorganic anion, and many have low volatility and high thermal stability. The free volume that results from the poor packing of the ions in the liquid typically leads to good solubility of $CO_2$.[20−23] $CO_2$ solubility in ILs is affected by the choice of cation and anion, with enhanced solubility observed with fluoroalkyl groups,[24] as well as the integration of amine functional groups which lead to chemisorption of $CO_2$, in addition to physisorption.[25−28] Such task-specific ionic liquids (TSILs) have demonstrated promising potential in DAC.[29,30] However, ILs suffer from high viscosity that impedes fast absorption rates of $CO_2$ and TSILs exhibit increase in viscosity upon $CO_2$ binding, limiting mass transport of $CO_2$.[31]

To overcome challenges associated with the viscosity and cost of TSILs, small molecule amines have been introduced to ILs for improved $CO_2$ absorption, providing both chemisorption pathways and low-volatility solvents for amines. For example, the addition of aqueous solutions of MEA and methyldiethanolamine (MDEA) with imidazolium-based ILs at 0−30 wt % concentrations was investigated.[32−34] Overall, the addition of aqueous amines to ILs showed a significant increase in absorption capacities compared to pure and aqueous ILs.[34] It was also evident that [BMIM][$BF_4$] represents a suitable cosolvent for the amines used for $CO_2$ capture, especially at lower temperatures and pressures.[33,34] Additionally, the performance of different binary mixtures of ILs and MEA was evaluated in the absence of water.[32,35,36] It is evident that IL mixtures with MEA can achieve competitive $CO_2$ absorption compared to that of aqueous amines. Further, loadings of MEA, up to 30 wt %, in [BMIM][$BF_4$], exhibits a high $CO_2$ capacity of 2.4 mol $CO_2$/kg of solvent at ambient conditions,[32] supporting that ILs can be used as nonvolatile solvents for amines. Notably, Pz's addition to alkanolamine mixtures with ILs, specifically mixtures of [BMIM][$BF_4$] and MEA, has been shown to increase the uptake rate and amount of $CO_2$ in the mixture.[36] The addition of small molecule amines and/or Pz to ILs can thus potentially enhance $CO_2$ uptake performance; however, such mixtures would still be limited by the volatility and corrosivity of amines,[16,37] as well as some ILs (e.g., [BMIM][$BF_4$], was shown to promote pitting corrosion in steel due to the presence of $F^-$ species).[38]

One approach to overcoming volatility and corrosivity of liquids for carbon capture is encapsulation in a $CO_2$-permeable shell. ILs have been encapsulated using microfluidic devices,[39,40] phase inversion,[41] or the soft-template approach[42−44] and these capsules find expanded application in contaminant removal,[43] microreactors,[45] and $CO_2$ capture.[46,47] The soft-template approach provides a scalable and tunable method to encapsulate a wide range of liquids of different physical properties, such as surface tension and viscosity. The soft-template method yields capsules tens of microns in diameter and up to 80 wt % of ILs.[48] Our groups previously demonstrated encapsulation of different ILs using a nonaqueous Pickering-emulsion and interfacial polymerization.[46,47,49] The resulting IL-filled capsules showed superior $CO_2$-sorption performance, with the IL in the core reaching full capacity in less time than the bulk IL and without the need for agitation.[46] Subsequent work demonstrated that the identity of the polyurea shell and residual amines impacts performance,[50] and that encapsulated TSILs are stable to different relative humidities, whereas zeolites lose their selectivity under similar conditions.[51] These works show that encapsulation of ILs offers the opportunity to enhance performance by tuning the core liquid, polymer shell, or both.

Herein, we report the encapsulation of a nontask-specific IL [BMIM][$BF_4$] mixed with reactive amines MEA and Pz and demonstrate that encapsulation mitigates amine evaporation and enhances mass transfer compared to the bulk liquid. The IL−amine mixtures are encapsulated in a polyurea shell using Pickering-emulsion template, with [BMIM][$BF_4$] chosen due to its low cost, ease of sourcing, and nonreactivity, as well as the fact that it has previously been mixed with MEA and Pz to give a $CO_2$-absorbing solvent with good performance. We posit that the encapsulation of $CO_2$ binding liquids can impede evaporation, a limitation of the bulk liquid, and that it can also enhance the effective surface area to increase the absorption rate.

## EXPERIMENTAL SECTION

### Materials

1-Butyl-3-methylimidazolium tetrafluoroborate ([BMIM][$BF_4$], 99%) was purchased from Iolitec. Monoethanolamine (MEA, 99%), hexamethylene diisocyanate (HDI, 99%), ethylenediamine (EDA, 99%), graphite flakes, and potassium permanganate ($KMnO_4$) were purchased from Sigma-Aldrich. Octane was purchased from Oakwood Chemical. Hydrogen peroxide ($H_2O_2$) in water (30 wt %) was purchased from Fisher Scientific. Sulfuric acid ($H_2SO_4$), *N*,*N*-dimethylformamide (DMF), piperazine (Pz, 99%), and 1-octadecylamine (97%) were purchased from Alfa Aesar. All chemicals were used as received.

### Synthesis of Alkylated GO (C18-GO)

Graphene oxide was synthesized using a modified Hummer's method,[52,53] as described in our previous reports.[54,55] The process entailed the oxidation of graphite with concentrated $H_2SO_4$ and $KMnO_4$ over a 96-h time frame, with the addition of $KMnO_4$ in four batches, once every 24 h. The mixture was then diluted, and aqueous $H_2O_2$ was added dropwise until the pink color disappeared. The resulting solid graphene oxide (GO) was purified through repeated washing with 2-propanol and centrifugation using a Thermo Scientific Sorvall ST8 and dried under reduced pressure. To synthesize alkylated GO, as-prepared GO was combined with octadecylamine in DMF at 50 °C until a dark precipitate formed. This precipitate was isolated and redispersed in toluene, and then additional octadecylamine was added, and the resulting mixture was stirred overnight at 50 °C. The nanosheets were washed with toluene, dried under reduced pressure, and finally dispersed in octane at a 2 mg/mL concentration.

### Preparation of Ionic Liquid/Amine Capsules

[BMIM][$BF_4$]/MEA (BM) liquid mixture was encapsulated using a similar approach as previously reported for neat IL.[42] [BMIM][$BF_4$] (363.8 mg, 1.61 mmol) was mixed with MEA (90.9 mg, 1.51 mmol) until homogeneous. EDA (0.07 mL, 1 mmol) was added to the mixture, and then the solution added to C18-GO dispersed in octane (2 mL, 2 mg/mL). The biphasic system was homogenized using a BioSpec Products hand-held emulsifier (Model 985370), undergoing three 20 s cycles with 15 s intervals between each cycle. Upon formation of the emulsion, it was diluted with 10 mL of octane. HDI (1 mmol, in 4 mL of octane) was added dropwise to the continuous phase. The polymerization was allowed to continue overnight and then quenched with propylamine (1 mL). The capsules were collected via gravity filtration, washed with excess octane, and dried under reduced pressure. The encapsulation of [BMIM][$BF_4$]/MEA/Pz (BMP) mixtures was performed in a similar manner, where Pz (25 mg, 0.29 mmol) was dissolved in [BMIM][$BF_4$] (337.4 mg, 1.49 mmol) and MEA (90.0 mg, 1.50 mmol), EDA (0.08 mL, 1.2 mmol) was added to the discontinuous phase, then emulsified with C18-GO in octane. HDI (1.2 mmol, in 4 mL of octane) was added dropwise after dilution of the emulsion with 10 mL of octane. The shell


https://doi.org/10.1021/acsaenm.4c00118
ACS Appl. Eng. Mater. 2024, 2, 1298−1305

formation and capsule isolation was performed as described for BM capsules.

### Analytical Methods

The capsules were imaged using an AmScope M150C and an AmScope MU500-CK 5.0 MP USB camera before and after isolation from the solvent. To prepare samples for optical microscopy, the capsules were deposited onto a glass slide. The capsules were gently compressed by placing them between two glass slides and separating the slides with a spacer to prevent crushing of the capsules. The resulting samples were then subjected to optical microscopy imaging. To determine the IL content in the capsules, 20 mg of capsules were mixed with a DMSO-d6 solution containing mesitylene as an internal standard (1 mL of 0.039 M). The mixture was analyzed by $^1$H NMR spectroscopy using a Bruker Ascend III HD 500 MHz NMR Magnet. The weight percentage of IL was calculated based on the relative integration of signals of the IL and mesitylene (see Supporting Information for detailed analysis). For SEM morphology analysis, a Tescan Vega SEM was used, where the isolated capsules were placed on double-sided carbon tape and loose particles were removed by blowing with a gentle nitrogen gas stream. For determining the size of the capsules, capsules were dispersed in octane, and a Partica LA-960S Laser Diffraction Particle Size Analyzer was used.

### $CO_2$ Uptake Measurements

$CO_2$ sorption/desorption was carried out using gravimetric thermal analysis using TA Instruments TGA 5500 and blending gas delivery module accessory for $CO_2/N_2$ gas switching. The weight of both the capsules and the unaltered liquid was stabilized under a nitrogen atmosphere at 75 °C prior to initiation of the absorption experiments. After the baseline stabilized, which indicated that all volatile components were eliminated, the temperature was lowered to 25 °C, and the gas was changed from nitrogen to carbon dioxide, and the absorption process was monitored until equilibrium, determined by a plateau in mass. Subsequently, the gas was switched back to nitrogen, and the temperature was raised to 75 °C for $CO_2$ desorption. The procedure was repeated after the baseline stabilized once again, and the temperature was allowed to return to 25 °C. The desorption temperature of 75 °C was the lowest temperature at which full desorption of $CO_2$ was observed.

Breakthrough experiments for DAC were performed following a previously described procedure.[51] Briefly, 0.25 ± 0.01 g of capsules was carefully packed into a 0.305 in. inner diameter column without capsule deformation. The column was equipped with a bypass to measure the feed composition. A mixture gas of 500 ± 5 ppm of $CO_2$ in $N_2$, provided as Airgas custom mixture, was fed through the bypass at 20 standard cubic centimeters per minute (sccm) via Brooks i5850, 0−200 sccm mass flow controller to calibrate the SBA-5, PP Systems, Inc. infrared gas analyzer. After 1 min, the feed gas was diverted to the sample column, and the effluent $CO_2$ concentration was measured over time. The experiment was stopped when the concentration of $CO_2$ in the effluent matched the feed concentration of 500 ± 5 ppm. Capacity analysis was performed by integrating the baseline subtracted breakthrough curve and using the following equation:

$$z = \frac{\int_0^t (C_0 - C)dt^*F}{W^*\hat{V}_{STP}} \quad (1)$$

where $z$ is the $CO_2$ loading in mmol $CO_2$/g of sorbent. $C_0$ is the dimensionless feed $CO_2$ composition (concentration in ppm * $10^6$), $C$ is the dimensionless effluent $CO_2$ composition, $t$ is time in minutes, $F$ is the total mass flow rate of the feed gas in sccm, $W$ is the weight of the sample, and $\hat{V}_{STP}$ is the molar volume of $CO_2$ at STP (22.4 scc $CO_2$/mmol $CO_2$, assuming ideal gas law in dilute conditions). Breakthrough time ($t_{BT}$) and pseudoequilibrium time ($t_{PE}$) are defined as the time at which the effluent concentration reached 25 ppm of $CO_2$ (5% of the feed concentration) and 490 ppm (97.5% of the feed concentration), respectively.

## RESULTS AND DISCUSSION

Microcapsules with a polymer-based shell and mixed core of the IL [BMIM][$BF_4$] and amine MEA, both with and without Pz, were synthesized from a Pickering-emulsion stabilized by alkylated nanosheets (i.e., C18-GO). Full experimental details of capsule preparation can be found in the experimental section. Two different types of capsules were prepared, using the same polymer shell but different core liquids: [BMIM]-[$BF_4$]/MEA (80/20 wt %) and [BMIM][$BF_4$]/MEA/Pz (75/20/5 wt %), referred to as BM and BMP, respectively. Briefly, nanosheets were dispersed in octane, and then the IL/amine mixture containing the monomer ethylene diamine (EDA) was added and sheer mixed, leading to the formation of droplets of IL/amine in octane, with the alkylated nanosheets stabilizing the fluid−fluid interface. To convert the emulsion droplets to capsules, the monomer hexamethylene diisocyanate (HDI) was added to the continuous octane phase of the emulsion, resulting in interfacial polymerization via an A2−B2 step growth polymerization of EDA with HDI at the interface. Optical microscopy images of BM and BMP capsules are shown in Figure S1A,B, respectively. The capsules were isolated by gravity filtration and imaged by optical microscopy (Figure S1C and S1E for BM and BMP, respectively); the isolated capsules were squished between two glass slides and imaged again, revealing that liquid is expelled from the capsule upon compression (Figure S1D and S1F for BM and BMP, respectively).

### Morphology

The capsules with a polyurea shell and core of [BMIM][$BF_4$]/MEA with and without Pz were imaged by scanning electron microscopy (SEM). As can be seen in Figure 1A, the surface of the BM capsules is rough which is consistent with the step growth polymerization used to produce the shell, as observed for previous capsules prepared by the soft template method.[50] Figure S2A shows an SEM image of a capsule that was

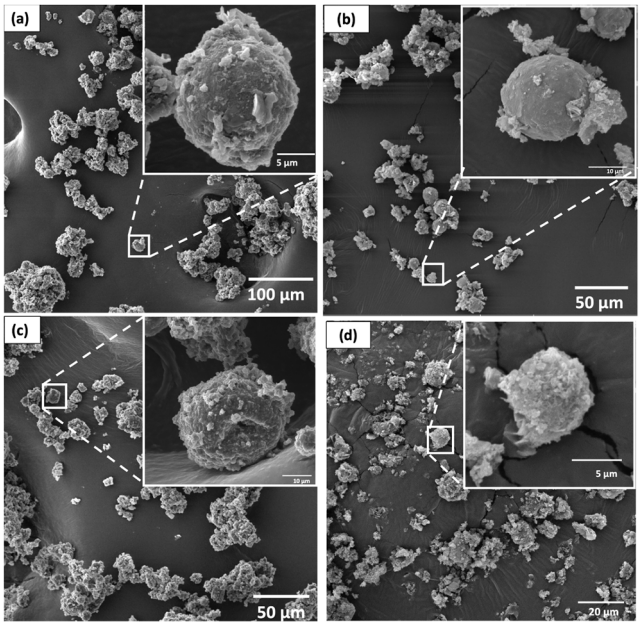


**Figure 1.** SEM images of (a) BM capsules; (b) hollow BM capsule shells after extraction of the core liquid; (c) BMP capsules; and (d) hollow BMP capsule shells after extraction of the core liquid.



https://doi.org/10.1021/acsaenm.4c00118
ACS Appl. Eng. Mater. 2024, 2, 1298−1305

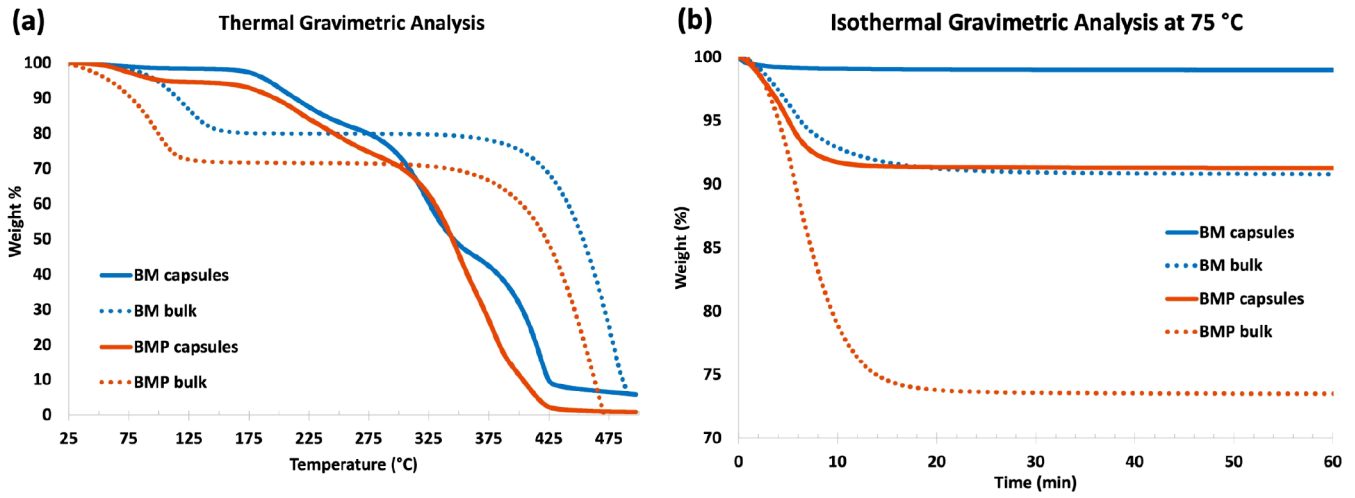


**Figure 2.** Weight loss profiles for BM capsules (solid blue), BM bulk mixture (dotted blue), BMP capsules (solid orange), BMP bulk mixture (dotted orange): (a) upon heating from ambient temperature to 500 °C with a 10 °C/min ramp and (b) isothermal heating at 75 °C.

fortuitously broken, allowing for the shell structure to be observed, where the shell thickness ranged from 0.3 to 1 $\mu$m; this is consistent with shell thickness previously reported for Pickering emulsion templated encapsulation.[46,56] Although some aggregation between capsules is observed, most are individual, supporting the desired high-accessibility surface area. The average diameter of the capsules was 27 $\mu$m in diameter with a standard deviation of ±24 $\mu$m, as determined by particle size analysis (Figure S2B). To quantify the capsule composition, the liquid core was extracted using deuterated dimethyl sulfoxide (DMSO-d6) containing an internal standard and then the liquid isolated by filtration and analyzed by $^1$H NMR spectroscopy. Integration of the peaks of the core liquid against the internal standard revealed that the BM capsules were 62 wt % core, consistent with the expected 66 wt % (Figure S3A, Table S1). The molar ratio of encapsulated [BMIM][$BF_4$]:MEA was determined to be 1.71:1, slightly higher than the initial pre-encapsulation ratio of 1.08:1, and thus the capsules were 53 wt % [BMIM][$BF_4$] and 9 wt % MEA. Decreased MEA content may be due to reaction of the primary amine with HDI, resulting in its incorporation into the polymer shell. Figure 1B shows the BM capsule shell after core extraction, demonstrating the integrity of the shell and that the spherical shape was maintained. Notably, sonicating the extracted shells in DMSO-d6 for 30 min led to extraction of an additional core liquid, as determined by $^1$H NMR (Figure S3D); as sonication breaks the capsule shell, the shell may be plasticized with the core liquid. The EDA peak was not observed, which confirms its consumption into the shell material.

The BMP capsules had similar surface roughness as the BM capsules, as shown in Figure 1C and had an average diameter of 33 ± 17 $\mu$m (Figure S2C). Extraction and characterization of the core by $^1$H NMR spectroscopy again verified the composition, and characterization of the hollowed BMP capsule shells showed they also remained spherical after extraction, as shown in Figure 1D. The core loading for BMP capsules was determined following a similar procedure as BM capsules, revealing the BMP capsules are 51 wt % core (Table S2); notably, acetone-d6 with an internal standard had to be used due to better solubility of Pz. The molar ratios of [BMIM][$BF_4$]:MEA:Pz used for emulsion formation was 1.00:0.98:0.17 and the molar ratios of the extracted core was 1.00:0.37:0.04 (Figure S3B), respectively. This means that the capsules are 46 wt % [BMIM][$BF_4$], MEA 5 wt %, and >1 wt % Pz. These data support that interfacial polymerization yields capsules with a polymer shell and a liquid core of IL and amines.

## Thermal Gravimetric Analysis and $CO_2$ Capacity

To assess the thermal stability of the capsules, weight loss of encapsulated and bulk liquid was examined using thermogravimetric analysis (TGA) and heating from ambient temperature to 500 °C at a rate of 10 °C/min (Figure 2A). Weight loss of the bulk liquid mixture began as the temperature increased above ambient temperature. The capsules, however, only started losing weight above 50 °C, and showed significant weight loss only above 150 °C. Thus, both BM and BMP capsules showed better thermal stability than their respective bulk liquids, which could thus be relevant to working conditions for $CO_2$ sorption and desorption.

To better understand the thermal stability of the encapsulated liquids under conditions relevant for $CO_2$ sorption and desorption, weight loss of the bulk and encapsulated liquids was evaluated isothermally at 25 and 75 °C over 1 h. At 25 °C, the bulk BM liquid showed steady weight loss over an hour, losing >5 wt %; in contrast, capsules of BM showed only 2 wt % loss over the same period, with a significantly less steep slope (see Figure S4A). Bulk BMP and its encapsulated counterpart both showed 8 wt % mass loss over an hour, with the BMP capsules showing a lower rate of weight loss compared to its bulk liquid. Notably, the capsules more rapidly lose mass in the initial 10 min, which may be attributed to volatile components on the capsule surface. As shown in Figure 2B, both types of bulk liquid lost significantly more weight than the encapsulated analogues at 75 °C. Bulk BM lost 14 wt % and bulk BMP lost 25 wt %, with weight loss for both plateauing after ∼17 min. In contrast, BM and BMP capsules lost ∼1 and 9 wt %, respectively, plateauing after <10 min of heating. Dissolving the liquid left in the TGA pan after these tests in acetone-d6 and characterization via $^1$H NMR analysis revealed that for the bulk liquids, MEA is no longer observed, supporting that when not encapsulated this component evaporates and leads to weight loss (Figure S3C).


https://doi.org/10.1021/acsaenm.4c00118
ACS Appl. Eng. Mater. 2024, 2, 1298−1305

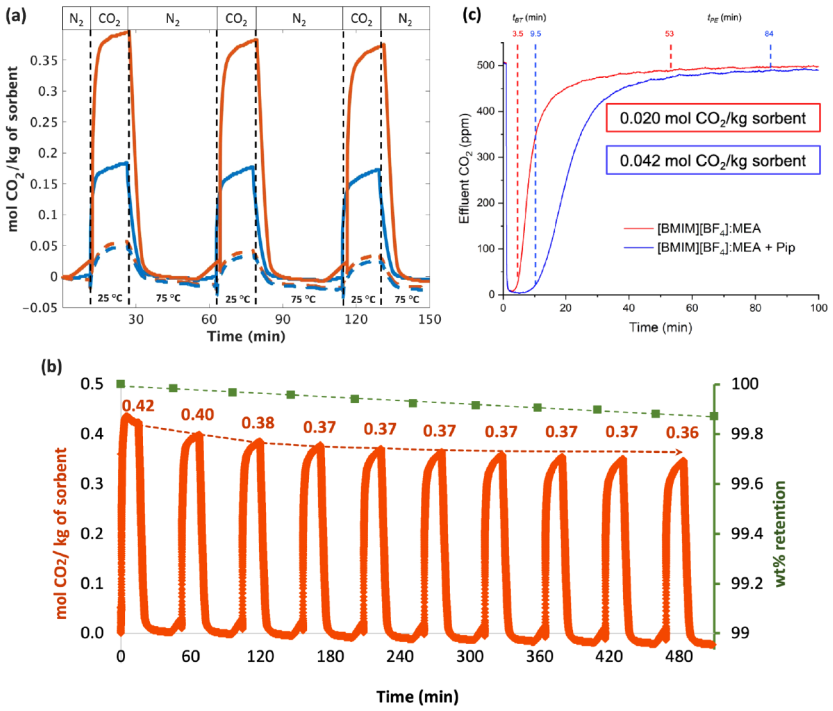


**Figure 3.** Gravimetric $CO_2$ uptake and release for (a) BM capsules (solid blue), BM bulk mixture (dotted blue), BMP capsules (solid orange), BMP bulk mixture (dotted orange), and (b) BMP capsules up to 10 cycles (solid orange). Green squares represent the wt % retention of the capsules after each cycle, and its linear fit (dashed green line). Absorption was performed at 25 °C and 1 bar with pure $CO_2$ purge at 25 mL/min rate for 15 min followed by desorption at 75 °C and pure $N_2$ purge for 30 min. (c) Breakthrough curves for BM and BMP capsules at under 500 ppm of $CO_2$ in $N_2$ at 25 °C. Breakthrough time ($t_{BT}$) and pseudoequilibrium time ($t_{PE}$) are denoted with red and blue vertical dashed lines for each curve, respectively.

To understand and evaluate the use of these IL/amine mixtures and their encapsulated derivative in carbon capture, $CO_2$ sorption−desorption cycling studies were performed, with sorption at 25 °C and desorption at 75 °C (Figure 3A). All samples were initially heated at 75 °C for 1 h and then cooled to room temperature under nitrogen to establish a baseline, followed by 1 cycle of $CO_2$ sorption−desorption. After this initial conditioning, capsules were exposed to $CO_2$ (at 1 bar) for 15 min based on the first cycle's duration until saturation. The gas was then switched to $N_2$ and the temperature was raised to 75 °C until a steady mass was observed, attributed to complete desorption of $CO_2$. This process was repeated three more times. Notably, 75 °C was the lowest temperature where full desorption was observed for the capsules, which is at least 25 °C lower than required for aqueous amine regeneration. This is attributed to both the lower heat capacity of [BMIM][$BF_4$] compared to water (1.61 vs 4.18 J/g/K at 25 °C)[57] and to the increased available area which increases desorption kinetics and provides a shorter path for $CO_2$ to diffuse out of the sorbents. Both the bulk liquids showed the same capacity of 0.05 mol $CO_2$/kg under the same conditions; this similar capacity is likely due to the loss of MEA, leaving only the IL behind; this capacity is slightly lower than prior reports for [BMIM][$BF_4$] of 0.07−0.09 mol $CO_2$/kg of sorbent at ambient temperature and 1 bar of $CO_2$,[22,58,59] and may be due to the limited surface area and lack of agitation of the liquid.

The $CO_2$ capacities for both BM and BMP capsules were significantly higher than the bulk liquids: BM capsules reached 0.2 mol $CO_2$/kg of sorbent and BMP capsules reached 0.4 mol $CO_2$/kg of sorbent. Pz is known to aid in the absorption rate of alkanolamines, and has also been reported it increase the solubility of $CO_2$ in [BMIM][$BF_4$]/amine mixtures.[36] Thus, BM capsules may not have reached full capacity due to limited $CO_2$ diffusion through the shell, but with the addition of Pz, a higher absorbance rate was observed, likely due to the increased kinetics of the reaction between MEA and $CO_2$ as observed for the BMP capsules. The increase in kinetics is attributed to Pz acting as a promotor in aqueous amines, and for [BMIM][$BF_4$] and MEA mixtures specifically, the rate constant increases as Pz's concentration increases, up to 10 wt %.[36] Under the same experimental conditions, both types of capsules showed a significantly higher $CO_2$ uptake rate than that of the bulk liquids. Their higher capacity suggests that MEA is preserved in the core and contributes to the $CO_2$ uptake as well as the amine-rich polymer shell that increases uptake capacity. These results help mitigate the main issue of the high volatility of amines in IL/amine mixtures for $CO_2$ uptake such that with encapsulation, fast reaction times are achieved, and volatile active components are preserved upon multiple cycles, which is critical in industrial applications.

$CO_2$ sorption/desorption was repeated over 10 cycles for BMP capsules, revealing excellent cyclability with less than 0.2 wt % loss at the end of the 10th cycle (Figure 3B). The weight loss during cycling was linear, losing 1.6 $\mu$g/cycle, with a starting weight of 12 mg of capsules at the beginning of the first cycle. By the end of the 10th cycle, only 0.13 wt % was lost throughout the cycling. Further, from the first to the fourth cycle, capacity decreased from 0.42 to 0.37 mol of $CO_2$/kg, but after this no further decrease in capacity was observed. These results suggest that after conditioning cycles, the composition of the capsules stabilized and more importantly, the mass loss


https://doi.org/10.1021/acsaenm.4c00118
ACS Appl. Eng. Mater. 2024, 2, 1298−1305

Table 1. Breakthrough Results for the Synthesized Capsules

| capsule core | breakthrough time (min) | pseudoequilibrium time (min) | pseudoequilibrium $CO_2$ capacity (mol $CO_2$/kg of sorbent) | $CO_2$:N ratio |
|---|---|---|---|---|
| BM | 3.5 | 53 | 0.020 | 0.013 |
| BMP | 9.5 | 84 | 0.042 | 0.043 |

is insignificant enough to cause the working capacity of the capsules to decrease, up to at least 10 cycles.

To establish the contribution of the polymer shell to $CO_2$ uptake, the absorption of the shell was also evaluated by preparing the same shells around a solid wax core (i.e., to have similar surface area). These capsules with a core of eicosane, a hydrocarbon wax, were synthesized using the same monomer system (see experimental for details). The capsules were pretreated by heating, and then the capacity was determined to be 0.025 mol of $CO_2$/kg (Figure S4B). Since the wax does not uptake $CO_2$, this capacity can be contributed to the shell itself. These results support the idea that the increased capacity after encapsulation of BM and BMP liquids is due to the preservation of volatile amines within the liquid core. It is also noteworthy that while EDA was used as the monomer for the interfacial polymerization, MEA and Pz can also reactive with HDI, thus the polymer shell itself is rich in secondary and tertiary amines, which have a lower $CO_2$-binding energy than primary amines, whichfurther lowers the regeneration cost.[60] Thus, the amine-rich polymer shell can support $CO_2$ capacity, and the capsule structure increases the available surface area of the encapsulated liquid.

To assess the kinetics of absorption in the capsules under conditions relevant to DAC, where the partial pressure of $CO_2$ is extremely low, breakthrough experiments were performed with a feed of 500 ppm of $CO_2$ in $N_2$ at 1 bar and 25 °C. The breakthrough curves are shown in Figure 3C and the related parameters are tabulated in Table 1. Consistent with the TGA results, the $CO_2$ capacity of the capsules with Pz is higher than the capsules without Pz, as discussed above.[36,61] By integration of the curve with eq 1, the obtained capacities are found to be lower than those measured by TGA at 1 bar of $CO_2$. This decreased capacity is expected with a decrease in the $CO_2$ partial pressure; however, considering the measured composition of the capsules, we find that the amine site utilization is low (~1%). The amines in MEA are expected to react with $CO_2$ at a ratio of 0.5:1 $CO_2$:N at high partial pressures of $CO_2$ like in flue gas (0.1 bar): for every amine that covalently bonds to $CO_2$, a second equivalent of amine serves as a base to neutralize the carbamate zwitterion formed.[62] In amine-tethered solid sorbents, a $CO_2$:N ratio of up to 0.2:1 has been reported at DAC conditions.[63] Using this ratio, the predicted capacity for the capsules without piperazine is 0.225 mol/kg. The most likely culprit for the observed reduction in capacity for the capsules is the viscosity increase experienced by MEA during $CO_2$ saturation upon formation of ammonium carbamate salts which increase intermolecular interaction strength.[64]

Initially, the $CO_2$ uptake is relatively fast due to the availability of MEA near the surface of the capsules. Once this MEA is saturated, the higher viscosity acts as a barrier for both the diffusion of MEA to the surface of the capsule and the diffusion of $CO_2$ through the core. Furthermore, the driving force for diffusion is concentration, and thus, at such low partial pressures, there is very little physically dissolved $CO_2$ in the IL to drive diffusion. It is also known that, at higher partial pressures, the ammonium carbamate salt formed upon $CO_2$ binding has a tendency to precipitate out of [BMIM][$BF_4$],[36] which would have a negative impact on $CO_2$ diffusion into the core, if also true for low partial pressures of $CO_2$. In the capsules with Pz, a similar trend of doubled capacity was observed at lower partial pressures compared to that of BM capsules. Although the capsules do not demonstrate competitive overall $CO_2$ capture performance under DAC relevant partial pressures, these results demonstrate that addition of Pz to IL amine solutions still enhances absorption, even at extremely low partial pressures, and that encapsulation in a polymer shell can be beneficial.

## CONCLUSION

The encapsulation of IL/amine mixtures was found to not only effectively mitigate the evaporation of volatile active amines of the liquid core but also significantly increase the absorption rate of $CO_2$. In the bulk, MEA evaporates in the desorption step due to its volatility, thus limiting the capacity of 0.05 mol of $CO_2$/kg of sorbent. This leads to a lower $CO_2$ uptaking potential of the bulk liquid. Upon encapsulation, volatile MEA is conserved within the capsule even after multiple absorption/desorption cycles, and hence, the uptake performance is maintained. An observed increase in the capacity by a factor of 8 compared to the bulk liquid, reaching 0.4 mol $CO_2$/kg of sorbent with Pz added to the mixture, confirms our hypothesis. This work demonstrates that encapsulating a $CO_2$ absorbing liquid in a solid−gas-permeable and robust polymeric shell increases available surface area, prevents volatilization of the amines, and increases absorption rates. The process requires no agitation to allow for a full sorption and desorption of $CO_2$, where such measures are crucial in industrial applications of volatile liquids like MEA. Although [BMIM][$BF_4$] does not significantly contribute to $CO_2$ absorption, this work serves as a proof of concept for future studies, where ILs with a higher affinity to $CO_2$ will be used in the same approach to make more cost-effective, highly selective, and easy-to-make materials for gas separation and storage purposes. Future work will focus on understanding diffusion mechanism of $CO_2$ through the shell, as well as optimizing the shell for a high $CO_2$ selectivity and permeability, allowing absorption at lower $CO_2$ concentration. This step is crucial toward tailoring materials for DAC applications to reach net-zero emissions.

## ASSOCIATED CONTENT

### Supporting Information

The Supporting Information is available free of charge at https://pubs.acs.org/doi/10.1021/acsaenm.4c00118.

Microscopic images of the capsules, SEM image of shell thickness and particle size analysis, $^1$H NMR spectra and wt % calculations, 25 °C gravimetric isotherm, and gravimetric shell uptake (PDF)

## AUTHOR INFORMATION

### Corresponding Author

**Emily Pentzer** − *Department of Materials Science and Engineering, Texas A&M University, College Station, Texas*



https://doi.org/10.1021/acsaenm.4c00118
ACS Appl. Eng. Mater. 2024, 2, 1298−1305

*77843, United States; Department of Chemistry, Texas A&M University, College Station, Texas 77843, United States;* orcid.org/0000-0001-6187-6135; Email: emilypentzer@tamu.edu

## Authors

**Luma Al-Mahbobi** − *Department of Materials Science and Engineering, Texas A&M University, College Station, Texas 77843, United States;* orcid.org/0000-0003-1216-6916

**Aidan Klemm** − *Department of Chemical Engineering Biomolecular Engineering, Case Western Reserve University, Cleveland, Ohio 44106, United States*

**Cameron Taylor** − *Department of Materials Science and Engineering, Texas A&M University, College Station, Texas 77843, United States*

**Burcu Gurkan** − *Department of Chemical Engineering Biomolecular Engineering, Case Western Reserve University, Cleveland, Ohio 44106, United States;* orcid.org/0000-0003-4886-3350

Complete contact information is available at: https://pubs.acs.org/10.1021/acsaenm.4c00118

## Notes

The authors declare no competing financial interest.

## ■ ACKNOWLEDGMENTS

The use of the Texas A&M University Microscopy and Imaging Center Core Facility (RRID:SCR 022128), and the Texas A&M University Soft Matter Facility (RRID SCR 022482) and contributions of Dr. Peiran Wei and Armaan Sanghvi are acknowledged. This material is based upon work supported by the U.S. Department of Energy (award no. DE-SC0022214).

## ■ REFERENCES

(1) Erans, M.; Sanz-Pérez, E. S.; Hanak, D. P.; Clulow, Z.; Reiner, D. M.; Mutch, G. A. Direct Air Capture: Process Technology, Techno-Economic and Socio-Political Challenges. *Energy Environ. Sci.* **2022**, *15*, 1360−1405.

(2) Kumar, S.; Srivastava, R.; Koh, J. Utilization of Zeolites as CO2capturing Agents: Advances and Future Perspectives. *J. CO2 Util.* **2020**, *41*, 101251.

(3) Cheng, Y.; Wang, X.; Jia, C.; Wang, Y.; Zhai, L.; Wang, Q.; Zhao, D. Ultrathin Mixed Matrix Membranes Containing Two-Dimensional Metal-Organic Framework Nanosheets for Efficient CO2/CH4 Separation. *J. Membr. Sci.* **2017**, *539*, 213−223.

(4) Ying, Y.; Cheng, Y.; Peh, S. B.; Liu, G.; Shah, B. B.; Zhai, L.; Zhao, D. Plasticization Resistance-Enhanced CO2 Separation at Elevated Pressures by Mixed Matrix Membranes Containing Flexible Metal-Organic Framework Fillers. *J. Membr. Sci.* **2019**, *582*, 103−110.

(5) Wang, B.; Sheng, M.; Xu, J.; Zhao, S.; Wang, J.; Wang, Z. Recent Advances of Gas Transport Channels Constructed with Different Dimensional Nanomaterials in Mixed-Matrix Membranes for CO2 Separation. *Small Methods* **2020**, *4*, 1900749.

(6) Mei, X.; Yang, S.; Lu, P.; Zhang, Y.; Zhang, J. Improving the Selectivity of ZIF-8/Polysulfone-Mixed Matrix Membranes by Polydopamine Modification for H2/CO2 Separation. *Front. Chem.* **2020**, *8*, 528.

(7) Lee, Y. Y.; Wickramasinghe, N. P.; Dikki, R.; Jan, D. L.; Gurkan, B. Facilitated Transport Membrane with Functionalized Ionic Liquid Carriers for CO2/N2, CO2/O2, and CO2/Air Separations. *Nanoscale* **2022**, *14* (35), 12638−12650.

(8) Bottoms, R. R.Process for Separating Acidic Gases US 1,783,901 A21930.

(9) Rochelle, G. T. Amine Scrubbing for CO2 Capture. *Science* **2009**, *325* (5948), 1652.

(10) Derks, P. W. J. *Carbon Dioxide Absorption in Piperazine Activated N- Methyldiethanolamine*; University of Twente: Netherlands, 2006. Ph.D. thesis. http://purl.utwente.nl/publications/57600

(11) Sharif, M.; Zhang, T.; Wu, X.; Yu, Y.; Zhang, Z. Evaluation of CO2 Absorption Performance by Molecular Dynamic Simulation for Mixed Secondary and Tertiary Amines. *Int. J. Greenhouse Gas Control* **2020**, *97*, 103059.

(12) Gao, T.; Rochelle, G. T. CO2 Absorption from Gas Turbine Flue Gas by Aqueous Piperazine with Intercooling. *Ind. Eng. Chem. Res.* **2020**, *59* (15), 7174−7181.

(13) Babu, A. S.; Rochelle, G. T. Energy Use of Piperazine with the Advanced Stripper from Pilot Plant Testing. *Int. J. Greenhouse Gas Control* **2022**, *113*, 103531.

(14) Narimani, M.; Amjad-Iranagh, S.; Modarress, H. CO2 Absorption into Aqueous Solutions of Monoethanolamine, Piperazine and Their Blends: Quantum Mechanics and Molecular Dynamics Studies. *J. Mol. Liq.* **2017**, *233*, 173−183.

(15) Scheiman, M. A.A review of monoethanolamine chemistry No. 5746; U. S. Naval Research Laboratory Report, 1962.

(16) Fischer, K. B.; Daga, A.; Hatchell, D.; Rochelle, G. T. *MEA And Piperazine Corrosion Of Carbon Steel And Stainless Steel. Energy Procedia* **2017**, *114*, 1751−1764.

(17) Malhotra, D.; Cantu, D. C.; Koech, P. K.; Heldebrant, D. J.; Karkamkar, A.; Zheng, F.; Bearden, M. D.; Rousseau, R.; Glezakou, V. A. Directed Hydrogen Bond Placement: Low Viscosity Amine Solvents for CO2 Capture. *ACS Sustainable Chem. Eng.* **2019**, *7*, 7535−7754.

(18) Wanderley, R. R.; Yuan, Y.; Rochelle, G. T.; Knuutila, H. K. CO2 Solubility and Mass Transfer in Water-Lean Solvents. *Chem. Eng. Sci.* **2019**, *202*, 403−416.

(19) Bougie, F.; Pokras, D.; Fan, X. Novel Non-Aqueous MEA Solutions for CO2 Capture. *Int. J. Greenhouse Gas Control* **2019**, *86*, 34−42.

(20) Husson-Borg, P.; Majer, V.; Costa Gomes, M. F. Solubilities of Oxygen and Carbon Dioxide in Butyl Methyl Imidazolium Tetrafluoroborate as a Function of Temperature and at Pressures Close to Atmospheric Pressure. *J. Chem. Eng. Data* **2003**, *48*, 480−485.

(21) Cadena, C.; Anthony, J. L.; Shah, J. K.; Morrow, T. I.; Brennecke, J. F.; Maginn, E. J. Why Is CO2 so Soluble in Imidazolium-Based Ionic Liquids? *J. Am. Chem. Soc.* **2004**, *126*, 5300−5308.

(22) Shiflett, M. B.; Yokozeki, A. Solubilities and Diffusivities of Carbon Dioxide in Ionic Liquids: [Bmim][PF6] and [Bmim][BF4]. *Ind. Eng. Chem. Res.* **2005**, *44*, 4453−4464.

(23) Soriano, A. N.; Doma, B. T.; Li, M. H. Carbon Dioxide Solubility in 1-Ethyl-3-Methylimidazolium Trifluoromethanesulfonate. *J. Chem. Thermodyn.* **2009**, *41*, 525−529.

(24) Muldoon, M. J.; Aki, S. N. V. K.; Anderson, J. L.; Dixon, J. K.; Brennecke, J. F. Improving Carbon Dioxide Solubility in Ionic Liquids. *J. Phys. Chem. B* **2007**, *111*, 9001−9009.

(25) Gurkan, B. E.; De La Fuente, J. C.; Mindrup, E. M.; Ficke, L. E.; Goodrich, B. F.; Price, E. A.; Schneider, W. F.; Brennecke, J. F. Equimolar CO2 Absorption by Anion-Functionalized Ionic Liquids. *J. Am. Chem. Soc.* **2010**, *132* (7), 2116−2117.

(26) Li, A.; Tian, Z.; Yan, T.; Jiang, D. E.; Dai, S. Anion-Functionalized Task-Specific Ionic Liquids: Molecular Origin of Change in Viscosity upon CO2 Capture. *J. Phys. Chem. B* **2014**, *118* (51), 14880−14887.

(27) Cui, G.; Wang, J.; Zhang, S. Active Chemisorption Sites in Functionalized Ionic Liquids for Carbon Capture. *Chem. Soc. Rev.* **2016**, *45*, 4307−4339.

(28) Keller, A. N.; Bentley, C. L.; Morales-Collazo, O.; Brennecke, J. F. Design and Characterization of Aprotic N-Heterocyclic Anion Ionic Liquids for Carbon Capture. *Chem. Eng. Data* **2022**, *67*, 375−384.

(29) Recker, E. A.; Green, M.; Soltani, M.; Paull, D. H.; Mcmanus, G. J.; Davis, J. H.; Mirjafari, A. Direct Air Capture of CO2via Ionic Liquids Derived from "Waste" Amino Acids. *ACS Sustainable Chem. Eng.* **2022**, *10* (36), 11885−11890.
(30) Lee, Y.-Y.; Cagli, E.; Klemm, A.; Park, Y.; Dikki, R.; Kidder, M. K.; Gurkan, B. Microwave Regeneration and Thermal and Oxidative Stability of Imidazolium Cyanopyrrolide Ionic Liquid for Direct Air Capture of Carbon Dioxide. *ChemSuschem* **2023**, *16* (13), No. e202300118.
(31) Gutowski, K. E.; Maginn, E. J. Amine-Functionalized Task-Specific Ionic Liquids: A Mechanistic Explanation for the Dramatic Increase in Viscosity upon Complexation with CO2 from Molecular Simulation. *J. Am. Chem. Soc.* **2008**, *130*, 14690−14704.
(32) Baj, S.; Siewniak, A.; Chrobok, A.; Krawczyk, T.; Sobolewski, A. Monoethanolamine and Ionic Liquid Aqueous Solutions as Effective Systems for CO2 Capture. *Chem. Technol. Biotechnol.* **2013**, *88* (7), 1220−1227.
(33) Ahmady, A.; Hashim, M. A.; Aroua, M. K. Absorption of Carbon Dioxide in the Aqueous Mixtures of Methyldiethanolamine with Three Types of Imidazolium-Based Ionic Liquids. *Fluid Phase Equilib.* **2011**, *309*, 76−82.
(34) Taib, M. M.; Murugesan, T. Solubilities of CO 2 in Aqueous Solutions of Ionic Liquids (ILs) and Monoethanolamine (MEA) at Pressures from 100 to 1600 kPa. *Chem. Eng. J.* **2012**, *181*−*182*, 56−62.
(35) Camper, D.; Bara, J. E.; Gin, D. L.; Noble, R. D. Room-Temperature Ionic Liquid-Amine Solutions: Tunable Solvents for Efficient and Reversible Capture of CO2. *Ind. Eng. Chem. Res.* **2008**, *47*, 8496−8498.
(36) Haider, M. B.; Hussain, Z.; Kumar, R. CO2 Absorption and Kinetic Study in Ionic Liquid Amine Blends. *J. Mol. Liq.* **2016**, *224*, 1025−1031.
(37) Du, Y.; Yuan, Y.; Rochelle, G. T. Volatility of Amines for CO2 Capture. *Int. J. Greenhouse Gas Control* **2017**, *58*, 1−9.
(38) He, S.; Qiu, Y.; Sun, Y.; Zhang, Z.; Cheng, J.; Gao, C.; Zhao, Z. Corrosion Behavior of AISI 1020 Steel in MEA and [Bmim]-BF4Mixed Solution Containing Saturated CO2. *Int. J. Greenhouse Gas Control* **2020**, *94*, 102931.
(39) Stolaroff, J. K.; Ye, C.; Oakdale, J. S.; Baker, S. E.; Smith, W. L.; Nguyen, D. T.; Spadaccini, C. M.; Aines, R. D. Microencapsulation of Advanced Solvents for Carbon Capture. *Faraday Discuss.* **2016**, *192*, 271−281.
(40) Stolaroff, J. K.; Ye, C.; Nguyen, D. T.; Oakdale, J.; Knipe, J. M.; Baker, S. E. CO2 Absorption Kinetics of Micro-Encapsulated Ionic Liquids. *Energy Procedia* **2017**, *114*, 860−865.
(41) Kaviani, S.; Kolahchyan, S.; Hickenbottom, K. L.; Lopez, A. M.; Nejati, S. Enhanced Solubility of Carbon Dioxide for Encapsulated Ionic Liquids in Polymeric Materials. *Chem. Eng. J.* **2018**, *354*, 753−757.
(42) Rodier, B.; De Leon, A.; Hemmingsen, C.; Pentzer, E. Controlling Oil-in-Oil Pickering-Type Emulsions Using 2D Materials as Surfactant. *ACS Macro Lett.* **2017**, *6*, 1201−1206.
(43) Luo, Q.; Wang, Y.; Chen, Z.; Wei, P.; Yoo, E.; Pentzer, E. Pickering Emulsion-Templated Encapsulation of Ionic Liquids for Contaminant Removal. *ACS Appl. Mater. Interfaces* **2019**, *11* (9), 9612−9620.
(44) Edgehouse, K.; Starvaggi, N.; Rosenfeld, N.; Bergbreiter, D.; Pentzer, E. Impact of Shell Composition on Dye Uptake by Capsules of Ionic Liquid. *Langmuir* **2022**, *38* (45), 13849−13856.
(45) Luo, Q.; Wei, P.; Huang, Q.; Gurkan, B.; Pentzer, E. B. Carbon Capsules of Ionic Liquid for Enhanced Performance of Electrochemical Double-Layer Capacitors. *ACS Appl. Mater. Interfaces* **2018**, *10* (19), 16707−16714.
(46) Huang, Q.; Luo, Q.; Wang, Y.; Pentzer, E.; Gurkan, B. Hybrid Ionic Liquid Capsules for Rapid CO2 Capture. *Ind. Eng. Chem. Res.* **2019**, *58* (24), 10503−10509.
(47) Luo, Q.; Pentzer, E. Encapsulation of Ionic Liquids for Tailored Applications. *ACS Appl. Mater. Interfaces* **2020**, *12* (5), 5169−5176.
(48) Hussain Solangi, N.; Hussin, F.; Anjum, A.; Sabzoi, N.; Ali Mazari, S.; Mubarak, N. M.; Siddiqui, M. T. H.; Saeed Qureshi, S. A Review of Encapsulated Ionic Liquids for CO2 Capture. *J. Mol. Liq.* **2023**, *374*, 121266.
(49) Starvaggi, N. C.; Bradford, B. J.; Taylor, C. D. L.; Pentzer, E. B. Wettability-Tuned Silica Particles for Emulsion-Templated Microcapsules. *J. Soft Matter.* **2023**, *19* (39), 7635−7643.
(50) Gaur, S. S.; Edgehouse, K. J.; Klemm, A.; Wei, P.; Gurkan, B.; Pentzer, E. B. Capsules with Polyurea Shells and Ionic Liquid Cores for CO2 Capture. *J. Polym. Sci.* **2021**, *59*, 2980−2989.
(51) Lee, Y. Y.; Edgehouse, K.; Klemm, A.; Mao, H.; Pentzer, E.; Gurkan, B. Capsules of Reactive Ionic Liquids for Selective Capture of Carbon Dioxide at Low Concentrations. *ACS Appl. Mater. Interfaces* **2020**, *12* (16), 19184−19193.
(52) Hummers, W. S.; Offeman, R. E. Preparation of Graphitic Oxide. *J. Am. Chem. Soc.* **1958**, *80*, 1339.
(53) Dimiev, A.; Kosynkin, D. V.; Alemany, L. B.; Chaguine, P.; Tour, J. M. Pristine Graphite Oxide. *J. Am. Chem. Soc.* **2012**, *134* (5), 2815−2822.
(54) Luo, Q.; Wang, Y.; Yoo, E.; Wei, P.; Pentzer, E. Ionic Liquid-Containing Pickering Emulsions Stabilized by Graphene Oxide-Based Surfactants. *Langmuir* **2018**, *34* (34), 10114−10122.
(55) Lak, S. N.; Hsieh, C.-M.; AlMahbobi, L.; Wang, Y.; Chakraborty, A.; Yu, C.; Pentzer, E. B. Printing Composites with Salt Hydrate Phase Change Materials for Thermal Energy Storage. *ACS Appl. Eng. Mater.* **2023**, *1* (8), 2279−2287.
(56) Wang, Y.; Wei, P.; Zhou, Q.; Cipriani, C.; Qi, M.; Sukhishvili, S.; Pentzer, E. Temperature-Dependent Capsule Shell Bonding and Destruction Based on Hindered Poly(Urea-Urethane) Chemistry. *Chem. Mater.* **2022**, *34* (13), 5821−5831.
(57) Waliszewski, D.; Stępniak, I.; Piekarski, H.; Lewandowski, A. Heat Capacities of Ionic Liquids and Their Heats of Solution in Molecular Liquids. *Thermochim. Acta* **2005**, *433*, 149−152.
(58) Anthony, J. L.; Anderson, J. L.; Maginn, E. J.; Brennecke, J. F. X. *J. Phys. Chem. B* **2005**, *109* (13), 6366−6374.
(59) Wang, M.; Zhang, L. Q.; Liu, H.; Zhang, J. Y.; Zheng, C. G. Studies on CO2 absorption performance by imidazole-based ionic liquid mixtures. *J. Fuel Chem. Technol.* **2012**, *40*, 1264−1268.
(60) Ko, Y. G.; Shin, S. S.; Choi, U. S. P. Primary, secondary, and tertiary amines for CO2 capture: Designing for mesoporous CO2 adsorbents. *J. Colloid Interface Sci.* **2011**, *361*, 594−602.
(61) Freeman, S. A.; Dugas, R.; Van Wagener, D. H.; Nguyen, T.; Rochelle, G. T. Carbon Dioxide Capture with Concentrated, Aqueous Piperazine. *Int. J. Greenhouse Gas Control* **2010**, *4* (2), 119−124.
(62) Li, K.; Cousins, A.; Yu, H.; Feron, P.; Tade, M.; Luo, W.; Chen, J. Systematic Study of Aqueous Monoethanolamine-Based CO2 Capture Process: Model Development and Process Improvement. *Energy Sci. Eng.* **2016**, *4* (1), 23−39.
(63) Choi, S.; Drese, J. H.; Eisenberger, P. M.; Jones, C. W. Application of Amine-Tethered Solid Sorbents for Direct CO 2 Capture from the Ambient Air. *Environ. Sci. Technol.* **2011**, *45*, 2420−2427.
(64) Amundsen, T. G.; Øi, L. E.; Eimer, D. A. Density and Viscosity of Monoethanolamine + Water + Carbon Dioxide from (25 to 80) °C. *J. Chem. Eng. Data* **2009**, *54* (11), 3096−3100.


https://doi.org/10.1021/acsaenm.4c00118
*ACS Appl. Eng. Mater.* 2024, 2, 1298−1305